HHS Public Access

Author manuscript

Gene Ther. Author manuscript; available in PMC 2015 April 30.

Published in final edited form as:

Gene Ther. 2015 January ; 22(1): 9–19. doi:10.1038/gt.2014.102.

SPARC (secreted protein acidic and rich in cysteine) knockdown protects mice from acute liver injury by reducing vascular endothelial cell damage

E Peixoto[1,10], **C Atorrasagasti**[1,2,10], **JB Aquino**[1,2], **R Militello**[3], **J Bayo**[1], **E Fiore**[1], **F Piccioni**[1], **E Salvatierra**[4], **L Alaniz**[1,2], **MG García**[1,2], **R Bataller**[5,6], **F Corrales**[7], **M Gidekel**[8,9], **O Podhajcer**[4], **MI Colombo**[2,3], and **G Mazzolini**[1,2]

[1]Liver Unit, Gene Therapy Laboratory, Facultad de Ciencias Biomédicas, Universidad Austral, Buenos Aires, Argentina

[2]CONICET (Consejo Nacional de Investigaciones Científicas y Técnicas), Buenos Aires, Argentina

[3]Facultad de Ciencias Médicas, Universidad Nacional de Cuyo, Mendoza, Argentina

[4]Molecular and Cellular Therapy Laboratory, Fundación Instituto Leloir, Buenos Aires, Argentina

[5]University of North Carolina at Chapel Hill, Chapel Hill, NC, USA

[6]Institut d'Investigacions Biomediques August Pi i Sunyer (IDIBAPS), Barcelona, Spain

[7]CIMA, Universidad de Navarra, Pamplona, España

[8]Universidad de la Frontera, Temuco, Chile

[9]Universidad Autónoma de Chile, Santiago, Chile

Abstract

Secreted protein, acidic and rich in cysteine (SPARC) is involved in many biological process including liver fibrogenesis, but its role in acute liver damage is unknown. To examine the role of SPARC in acute liver injury, we used SPARC knock-out ($SPARC^{-/-}$) mice. Two models of acute liver damage were used: concanavalin A (Con A) and the agonistic anti-CD95 antibody Jo2. SPARC expression levels were analyzed in liver samples from patients with acute-on-chronic alcoholic hepatitis (AH). SPARC expression is increased on acute-on-chronic AH patients. Knockdown of SPARC decreased hepatic damage in the two models of liver injury. $SPARC^{-/-}$ mice showed a marked reduction in Con A-induced necroinflammation. Infiltration by CD4+ T cells, expression of tumor necrosis factor-α and interleukin-6 and apoptosis were attenuated in $SPARC^{-/-}$ mice. Sinusoidal endothelial cell monolayer was preserved and was less activated in

Correspondence: Professor G Mazzolini, Liver Unit, Gene Therapy Laboratory, Facultad de Ciencias Biomédicas. Universidad Austral, Avenue Presidente Perón 1500 (B1629ODT), Derqui-Pilar, Buenos Aires 1635, Argentina. gmazzoli@cas.austral.edu.ar.

[10]These authors contributed equally to this work.

CONFLICT OF INTEREST

The authors declare no conflict of interest.

Supplementary Information accompanies this paper on Gene Therapy website (http://www.nature.com/gt)

Con A-treated SPARC$^{-/-}$ mice. SPARC knockdown reduced Con A-induced autophagy of cultured human microvascular endothelial cells (HMEC-1). Hepatic transcriptome analysis revealed several gene networks that may have a role in the attenuated liver damaged found in Con A-treated SPARC$^{-/-}$ mice. SPARC has a significant role in the development of Con A-induced severe liver injury. These results suggest that SPARC could represent a therapeutic target in acute liver injury.

INTRODUCTION

Acute liver injury might be caused by a number of etiologies including viral, toxic and autoimmune, among others.[1] Liver damage may progress to acute liver failure when the amount of hepatocyte death overwhelmed the liver's regenerative capability.

Secreted protein, acidic and rich in cysteine (SPARC), also called as osteonectin or BM-40, is a secreted extracellular matrix-associated protein involved in a number of biological processes.[2] Among other functions, SPARC has a major role in wound healing response to injury, tissue remodeling[3] and fibrosis.[4,5] Regarding the role of SPARC in liver fibrosis, we[4] and others[6] showed that SPARC is overexpressed in cirrhotic livers form mice and patients. Mechanisms behind the inhibition of fibrosis when SPARC is knocked down involved reduction of transforming growth factor-β1 (TGF-β1) expression and a decreased number of activated hepatic stellate cells. In addition, SPARC has the ability to induce actin cytoskeletal rearrangement essential for cell transmigration by binding to vascular cell adhesion molecule-1 (VCAM-1)[7] and it can also exert counter-adhesive function by affecting focal adhesion complexes and reorganization of actin stress fibers.[8] We recently found that SPARC is involved in hepatic fibrogenesis using a chronic damage model.[4] To examine the role of SPARC in acute liver injury we used SPARC knockout mice and explored two different models of acute liver injury induced by concanavalin A (Con A) and the agonistic CD95 antibody Jo2.

Con A is a lectin which is known to activate T-cell populations.[9] Con A induces acute inflammation of the liver parenchyma by the infiltration of activated lymphocytes, resulting in massive hepatocellular necrosis and intra-sinusoidal hemostasis. Con A-induced severe liver injury is being extensively used as an acute model for human autoimmune hepatitis as it mimics several features of this disease. It has been observed that Con A can induce both T-cell-dependent and -independent hepatitis in mice.[10,11] Mechanisms of T-cell-independent liver damage likely involve autophagy of hepatic endothelial cells and hepatocytes, although underlying events explaining such organ/cellular specificity is still unclear.[11] Acute liver damage can also be induced by the agonistic anti-CD95 antibody Jo2 that generates apoptosis on hepatocytes and liver endothelial cells.[12,13]

Mice with a knockout of SPARC exhibited significantly decreased sensitivity toward acute liver damage induced by the agonistic CD95 antibody Jo2 and Con A. In this work, we provide for the first time strong evidences that SPARC deficiency has a protective role in Con A-induced hepatitis model likely through reducing vascular endothelial cell susceptibility to apoptosis/autophagy and subsequent hepatic necro-inflammation. This

report further supports the design of new therapeutic approaches based on SPARC expression inhibition for the treatment of acute liver injury.

RESULTS

Expression of SPARC during severe liver injury and decreased liver damage in SPARC-deficient mice

A significant upregulation in SPARC expression levels was observed in samples from patients with alcoholic hepatitis (AH) when compared with patients with chronic hepatitis C virus infection or nonalcoholic steatohepatitis by quantitative PCR (qPCR) (Figure 1a). We next asked whether SPARC expression could be similarly induced in *in vivo* models developed in $SPARC^{+/+}$ mice based on single Con A, anti-CD95 or galactosamine/lipopolysaccharide treatment. Although in non-treated animals SPARC expression was almost negligible, after 24 h of Con A, anti-CD95 or galactosamine/lipopolysaccharide treatment, SPARC was upregulated as measured by qPCR. Immunohistochemistry analysis of Con A-treated mice revealed that SPARC was mainly expressed in sinusoid areas (Figure 1b). We then asked whether SPARC deficiency may affect hepatocyte death and inflammation during acute liver injury. At 24 h after Con A (Figure 1c) or anti-CD95 (Figure 1d) administration, $SPARC^{+/+}$ livers showed extensive areas of necrosis, inflammation and distortion of liver architecture. These features were markedly reduced in livers from Con A or anti-CD95-treated $SPARC^{-/-}$ animals. Then, serum transaminases levels were measured at 24 h after Con A or anti-CD95 treatment. A significant increase in aspartate transaminase and alanine transaminase serum levels were found in $SPARC^{+/+}$ mice in comparison with $SPARC^{-/-}$ mice on both models (Figures 1c and d). Similar results were observed in Galactosamin/lipopolysaccharide animal model (not shown).

To assess whether hepatic SPARC-induced *in vivo* inhibition could protect against Con A-induced liver damage, AdasSPARC or Adβgal (control adenovirus) were infused *via* the tail vein 48 h prior to Con A application in wild-type (wt) mice. AdasSPARC was able to attenuate hepatic SPARC expression as shown by qPCR (Figure 2a) and markedly decreased liver injury.

To further evaluate the therapeutic effect of SPARC inhibition once liver injury was induced, small interference RNA anti-SPARC (siSPARC) was administered via portal vein 2 h after Con A injection. Forty-eight hours after siSPARC injection a significant decrease in liver damage was observed in comparison with siControl (Figure 2c). In addition, siSPARC was able to attenuate hepatic SPARC expression as shown by qPCR (Figure 2b) and, most important, therapeutic inhibition of SPARC resulted in prolonged animal survival (Figure 2d). When heterocygotic SPARC animals ($SPARC^{+/-}$) were treated with Con A decreased amount of liver damage was observed in comparison with Con A-treated $SPARC^{+/+}$ mice (Figure 2e). In addition, when SPARC expression was reconstituted with an adenovirus encoding SPARC (AdsSPARC) sensitivity to Con A was partially restored (Figure 2f).

Consistent with results shown in Figures 1 and 2, a significant reduction in the hepatic inflammation was found after Con A application in $SPARC^{-/-}$ when compared with wt mice

(Figures 3a and b). A significant reduction in the amount of $CD4^+$ T lymphocytes was observed in $SPARC^{-/-}$ mice when compared with control (Figures 3c and d).

We then analyzed the effect of SPARC inhibition on serum concentration of pro-inflammatory cytokines after Con A injection. As shown in Figure 3e, serum levels of interleukin-6 and TNF-α were significantly reduced in $SPARC^{-/-}$ mice at 3 and 9 h after Con A application, respectively. In addition, a lack of TGF-β1 peak was found in SPARC-deficient mice when compared with $SPARC^{+/+}$ at 9 and 24 h (Figure 3e). Furthermore, a reduction in the extent of liver parenchymal cell apoptosis was found in $SPARC^{-/-}$ when compared with wt mice by TUNEL (Figure 3f).

Reduced endothelial cell damage after SPARC knockdown

Alterations in liver sinusoidal endothelial cells (LSECs) are likely among the earliest events of severe liver injury facilitating infiltration of activated T cells into liver parenchyma. By electron microscopy, LSEC layer was observed to be disrupted in $SPARC^{+/+}$ mice, but it remained preserved in $SPARC^{-/-}$ mice (Figure 4a). To uncover the mechanisms by which Con A alters endothelial cell barrier, we performed culture experiments with human microvascular endothelial cell (HMEC-1) cells. SPARC mRNA expression was induced after 1 h of Con A incubation (Figure 4b). To assess the role of SPARC deficiency in endothelial cells, SPARC was knocked down by using a lentivirus encoding a siRNA specific for SPARC (Figure 4c). A significant reduction in both the proportion of adhered cells with a thick fibrillar pattern, known as stress fibers and in the phalloidin staining distribution, as well as an increased in gaps separating cells were found in cultures of naive and siSCR-treated cells when compared with SPARC siRNA-treated cells (Figure 4d). Interestingly, SPARC knockdown resulted in a significant reduction in the percentage of apoptotic cells after 3 h of Con A incubation (Figure 4e). SPARC knockdown also showed an increased HMEC-1 adhesive capacity to fibronectin (not shown).

Next, we assessed if SPARC knockdown decreases the amount of transmigrated lymphocytes through Con A-treated HMEC-1 cell layer toward CCL19 and CCL21 as chemoattractants. SPARC inhibition resulted in a reduction in the number of lymphocytes that migrated across the endothelial cell monolayer (Figure 4f). These data suggest that SPARC inhibition might protect endothelial cell layer from apoptosis induction caused by Con A and preserve endothelial cell monolayer.

Because expression of VCAM-1 in endothelial cells is induced by inflammation,[14] we next analyzed its expression pattern after Con A application. As expected, a marked upregulation of VCAM-1 was found in the liver of wt mice at 7 h after Con A application that was marked blunted in $SPARC^{-/-}$ mice (Figure 4g). These results further suggest the involvement of SPARC in sinusoidal cells inflammation in early development of severe liver injury.

To further understand how the endothelial layer could be affected by Con A resulting in subsequent hemorrhage and massive cellular infiltration, HMEC-1 cells were stained with the autophagic marker LC3. As shown in Figure 4h, the LC3 punctate pattern was increased in HMEC-1 cells after 3 h of Con A incubation. Interestingly, SPARC knockdown prevented

LC3 staining. Blocking autophagy using chloroquine confirmed that LC3 decrease with SPARC knockdown resulted from autophagy inhibition as LC3 dots remained stable and not accumulated when SPARC was attenuated and the LC3 flux interrupted. These results indicate that Con A induces autophagy in endothelial cells, which is partially mediated by SPARC.

Transcriptome analysis reveals molecular mechanisms potentially involved in the role of SPARC in Con A-induced severe liver damage

Microarray analysis was performed in liver tissue from SPARC$^{-/-}$ and SPARC$^{+/+}$ mice at 9 h after Con A administration. A total of 169 genes showed changes ($P < 0.01$; 94 upregulated and 75 down-regulated genes) in SPARC$^{-/-}$ mice when compared with wt (Table 1). A list of the significantly modified genes as classified by ontological biological process categories is shown in supplementary table. Interestingly, canonical pathways and biological functions identified by Ingenuity Pathway Analysis showed key groups of genes associated with cell adhesion, cytoskeletal organization and apoptosis (Figure 5). They include upregulation of actin capping protein β2 (*CAPZB*, NM_009798) gene, tubulin β Class IIb (*TUBB2B*, NM_023716) and downregulation of thymosin β (*TMSB10*, NM_001190327), slingshot homolog 1 (*SSH1*, NM_198109), thioesterase superfamily member 4 (*THEM4*, NM_029431), tumor necrosis factor receptor superfamily member 14 (*TNFRSF14*, NM_178931) and potassium voltage-gated channel, KQT-Like subfamily member 1 (*KCNQ1*, NM_008434).

DISCUSSION

In this work, we demonstrated that SPARC expression were strongly upregulated in the liver of patients with AH, but not in non-cirrhotic patients with chronic hepatitis C virus infection or nonalcoholic steatohepatitis, indicating that SPARC might be involved in the physiopathology of acute-induced liver damage. In agreement with this, Bykov *et al.*[15] observed that SPARC is induced in mice with AH using microarray analysis. Our results showed that SPARC expression was also induced in two additional models of acute liver damage induced by the agonistic CD95 antibody Jo2 and Con A *in vivo*.

We herein showed that acute liver damage was dramatically reduced in livers from Con A-treated SPARC$^{-/-}$ animals. Consistent with this result, *in vivo* attenuation of SPARC expression AdasSPARC was efficient to prevent Con A-induced acute hepatitis, underlying a key contribution of SPARC in this model. In addition and more importantly, *in vivo* SPARC inhibition using siSPARC administered after the initiation of Con A-induced liver damage resulted therapeutic, decreased liver injury and prolonged animal survival. This model is characterized by an excessive production of pro-inflammatory cytokines that is followed by a massive inflammatory infiltration and hepatic necrosis. When we analyzed the effect of SPARC knockdown on serum concentration of interleukin-6 and tumor necrosis factor-α (TNF-α) after Con A injection significantly reduced levels were observed compared with SPARC$^{+/+}$ mice. This observation reveals that the protective effect of SPARC knockdown is related, at least in part, to a less inflamed microenvironment.

TGF-β is a pleiotropic cytokine with a crucial role in acute liver injury and in the induction of apoptotic cell death in hepatocytes, although the mechanisms of apoptosis triggered by TGF-β are diverse,[16] cooperation with FasL or TNF-α at inducing hepatocyte apoptosis was reported. Interestingly, SPARC$^{-/-}$ mice treated with Con A showed a significant decrease in the expression of TGF-β1 when compared with SPARC$^{+/+}$ mice. Thus, a protective effect of SPARC deficiency would likely be related to a modulation in the TGF-β1 upregulation induced by Con A.

Lymphocyte migration to the subendothelial layer is a common feature of inflammatory human liver diseases such as immune-mediated hepatitis. A critical reduction in the hepatic inflammation composed by CD8$^+$ (not shown) and CD4$^+$ T lymphocytes was seen after Con A injection in SPARC$^{-/-}$ mice. This result is in line with our previous report showing that CD4$^+$ T cells from SPARC$^{-/-}$ mice showed a decreased migratory ability toward inflamed livers.[4] This effect might contribute to decrease the degree of activated lymphocytes infiltrating the liver.

The inflammation and damage of hepatic vascular endothelial cells will precede the subsequent lymphocyte infiltration and cytokine-mediated hepatocyte injury. It was observed that Con A injection induced expression of a wide variety of chemokines and adhesion molecules in the liver including VCAM-1. A potent upregulation of VCAM-1 was seen in the liver of wt mice after Con A injection, whereas in SPARC$^{-/-}$ mice sinusoidal inflammation is markedly diminished providing evidence that the absence of SPARC might be involved in preservation of sinusoidal barrier. Con A was shown to bind to LSECs early after its application *in vivo*[17] and activated T cells in presence of Con A was found to result in LSEC cytotoxicity. Because the damage of hepatic vascular endothelial cells precedes the subsequent lymphocyte infiltration and cytokine-mediated hepatocyte injury we analyzed the LSEC layer by electron microscopy and observed that it was disrupted in SPARC$^{+/+}$ mice, but remained well preserved in SPARC$^{-/-}$ mice. Cell adhesive properties require secreted extracellular matrix-dependent intracellular signaling pathways and they are usually accompanied by dynamic changes in actin filament cytoskeleton. Considering that SPARC expression is known to influence cell adhesiveness and that SPARC mediates focal adhesion disassembly in bovine aortic endothelial cells,[8] we analyzed the effects of Con A on HMEC-1 cells. In agreement with other reports, SPARC inhibition resulted in an increased HMEC-1 adhesion, well cytoskeleton organization and reduced transmigration of activated lymphocytes after Con A treatment. These results suggest that SPARC absence may be beneficial to keep the endothelial barrier preserved to ameliorate the hepatic injury.

It has previously shown that Con A might induce autophagy of LSEC.[11] Consistent with our results, the disruption of endothelial cells may be mechanistically explained in part by the fact that Con A can induce endothelial damage independent of T cells through autophagy mediated apoptosis as previously evaluated in severe combined immunodeficiency/non-obese diabetic mice and HMEC-1 cell culture.[10,11] In addition, it has been reported that SPARC potentiates apoptosis through caspase 8 in colorectal cancer cells[18] and induces apoptosis in ovarian cancer cells.[19] The inhibition of SPARC reported on this work was successful to decrease autophagic and apoptotic rates induced by Con A.

Microarray analyses showed a number of genes that were narrowed down. Our overall results suggest that the reduction in liver damage observed in SPARC-deficient mice seems to be the result of a sum of several mechanisms rather than the effect of changes in a small group of specific genes. In accordance with phalloidin results, we observed the increased expression of CAPZB and tropomyosin 4 (*TPM4*, NM_001001491) that stabilizes actin filaments and has a role in the regulation of cell morphology and cytoskeletal organization. This result agrees with Bhoopathi *et al.*[20] that reports SPARC as an effector of Scr-induced cytoskeleton disruption in meduloblastoma cells. Our best Ingenuity Pathway Analysis gene network model showed that SPARC depletion was associated with an upregulation of *CAPZB* gene, involved in the regulation of cell morphology and cytoskeletal organization,[21] and *TUBB2B*, a major component of microtubules. In contrast, results showed downregulation of *TMSB10* that regulates actin dynamics as a cytoplasm G-actin-sequestering protein leading to actin disruption and apoptosis in cancer cells.[22] In addition, the protein encoded by *SSH1* gene dephosphorylates and activates the actin binding/depolymerizing factor cofilin, which subsequently binds to actin filaments and stimulates their disassembly;[23] this gene is down-regulated in SPARC$^{-/-}$ mice. Another important gene found downregulated is *TNFRSF14*, a member of the TNF-receptor super-family, which may mediate the signal transduction pathways that activate the immune response triggered by Con A administration.[24]

In summary, we herein demonstrate that SPARC deficiency protects the liver from Con A and the agonistic anti-CD95 receptor antibody Jo2-induced liver injury. Importantly, therapeutic inhibition of SPARC resulted in a reduced liver damage and prolonged animal survival. Mechanisms involved in Con A model are complex and likely act at different levels and through diverse processes implicated in hepatic damage.

Our new evidences implicate reduction in the extent of liver necro-inflammation, reduction in endothelial cell apoptosis and restoration of their adhesive properties with the result of an intact endothelial cell layer that prevents CD4 T-cell transmigration through the endothelial layer. The differential gene expression pattern suggests protection against cytoskeletal disruption making endothelial cells less susceptible to Con A-induced damage. In conclusion, the design of interventions to inhibit hepatic SPARC would likely help protecting the liver against acute liver injury.

MATERIALS AND METHODS

Animals and experimental design

Male C57BL/6x129SvJ SPARC$^{-/-}$, SPARC$^{+/+}$ or SPARC$^{+/-}$ littermate mice (6–8 weeks old) were used (the Jackson Laboratory, Bar Harbor, ME, USA). Mice were given a single i.v. injection of Con A (Sigma, St Louis, MO, USA) at 15 μg g^{-1} bodyweight. Animals were killed at 3, 9 and 24 h after Con A application and samples were obtained. Some groups of animals received i.v. administration of 1.3×10^9 median tissue culture infective dose (TCID50) of AdasSPARC or Adβgal adenoviruses. Other groups received intrahepatic administration of AdsSPARC or Adβgal (TCID50: 5×10^9).

For a therapeutic use of siRNA, rat SPARC siRNAs (siSPARC; four constructs used in combination: 5′-GAGAAGAACUACAACAUGUUU-3′, 5′-CCAGAACCAUCAUUGCAAAUU-3′, 5′-GAACAUUGCACCACUCGCUUU-3′, 5′-CUACAUCGGACCAUGCAAAUU-3′) and a control siRNA (siControl; D-001210-05-05) were purchased from Dharmacon (Chicago, IL, USA). Mice were given a single i.v. injection of Con A (Sigma) at 10 μg g^{-1} body weight. Some groups of animals received via portal vein 1 ml of saline, siControl or siSPARC. Sham-operated animals did not receive Con A. Animals were killed at 48 h after Con A application and samples were obtained. Some animals were used for survival analysis. Other group of animals received a sub-lethal dose (0,25 μg g^{-1}) of the agonistic CD95 antibody Jo2 or D-Galactosamin/lipopolysaccharide (galactosamin; 0,125 mg g^{-1} per lipopolysaccharide; 12.5 μg kg^{-1}) and killed at 24 h. All experiments were performed according to the ‘Guide for the Care and Use of Laboratory Animals’ and approved by the School of Biomedical Sciences of Austral University. Patients admitted to the Liver Unit, Hospital Clínic of Barcelona with clinical, analytical and histological features of AH from 2007 to 2010 were included in the study. All patients had histological diagnosis of AH (n = 34). Liver biopsy was obtained using a transjugular approach. We included a cohort of patients with morbid obesity and associated nonalcoholic steatohepatitis (n = 10). A laparoscopic liver biopsy was obtained in these patients during bariatric surgery. We also included patients with chronic hepatitis C-induced liver disease who did not receive previous antiviral treatment (n = 5). As controls, fragments of normal liver tissue were obtained from optimal cadaveric liver donors (n = 3) or resection of liver metastases (n = 3). The study protocol conformed to the ethical guidelines of the 1975 Declaration of Helsinki and was approved by the Ethics Committee of the Hospital Clinic of Barcelona. All patients gave informed consent. For in vitro studies Con A and chloroquine was administered on media at a concentration of 15 μg ml^{-1} and 20 μM respectively.

Generation of recombinant vectors

AdasSPARC, an adenovirus encoding for SPARC antisense full-length sequence, AdsSPARC, an adenovirus encoding for the sense full-length sequence[25] and Adβgal were constructed and produced as described elsewhere.[26] Lentivirus vectors were produced as follows. pRNATin.H1.4-L.51 vector containing siSPARC sequence (tggatcccgcggcaggcagagcgcgct ctcttgatatccggagagcgcgctctgcctgccgttttttccaactcgagg) was produced following the Genscript cloning protocol. Scramble control vector was ordered from Genscript. Lentiviral vectors were produced using The ViraPower Lentiviral Technology (Invitrogen, Carlsbad, CA, USA). Briefly, 293 FT cells were transfected with a mixture of 36 μl Lipofectamine 2000 (Invitrogen), 9 μg (9 μl) of ViraPower Packaging Mix and 3 μg of the pRNATin.H1.4-L.51 (siSPARC) or scramble (siSCR) expression plasmid DNA in 1 ml of Opti-MEM I Medium (Invitrogen) without serum. Lentivirus-containing supernantants were collected after 48–72 h post transfection. Supernantant was used for 48 h to transduce HMEC-1 cells.

Serological analysis

Serum was obtained by retro-orbital bleeding from anesthetized mice and analyzed using a standard clinical analyzer (ARCHITECT, Abbott, Abbott Park, IL, USA). Serum levels of

TNF, and interleukin-6 were measured by enzyme-linked immunosorbent assay using ELISA kits (R&D Systems, Minneapolis, MN, USA) according to manufacturer's instructions.

qPCR

Liver tissue was homogenized and total RNA was extracted by trizol reagent (Sigma). RNA (1 μg) was reverse transcribed with 200 U of superscript ii reverse transcriptase (Invitrogen) using 500 ng of oligo (dT) primers. cDNAs were subjected to qPCR (Table 2). SPARC and TGF-β1 mRNA levels were quantified by SYBR Green (Invitrogen) qPCR (Stratagene Mx3005p, Stratagene, USA). All PCR amplifications were carried out using 40 cycles of 95 °C for 30 s, 55 °C for 30 s and 72 °C for 30 s. For liver human biopsies, qPCR reactions were carried out in a StepOnePlusTM Real-Time PCR System using commercial primer-probe pairs (Applied Biosystems, Foster City, CA, USA). mRNA levels for human SPARC were measured. 18S RNA was used as the endogenous control. Gene expression values were calculated based on the ΔΔCt method. The results were expressed as $2^{-\Delta\Delta Ct}$ referred as fold increase compared with the mean expression quantified on normal livers.

Histological analysis and immunostaining

Liver samples were fixed in 10% formalin and then paraffin-embedded. Tissue was dehydrated, embedded in paraffin and stained by hematoxylin and eosin. Chromogenic immunohistochemistry for SPARC and CD4 was performed as described elsewhere.[4] In fluorescent immunocytochemistry, cultured HMEC-1 cells, siSPARC lentivirus transfected or siSCR (scrambled siRNA lentivirus-infected cells) were stained with anti-LC3 antibody (1:50, Abgent, San Diego, CA, USA), using an anti-rabbit Alexa 488–conjugated IgG secondary antibody (1:200, Promega, Madison, WI, USA). For *in situ* detection of apoptotic cells, terminal deoxynucleotidyl transferase-mediated labeling of nick-end DNA (TUNEL) staining was performed on cryosections, according to manufacturer's instructions (Calbiochem, Darmstadt, Germany). In fluorescent immunohistochemistry, frozen liver sections were stained using an anti-VCAM (1:25, BD, Franklin Lakes, NJ, USA) primary antibody and an anti-rat Cy3-conjugated IgG secondary antibody (1:400, Jackson Immunoresearch, West Grove, PA, USA).

For *in vitro* studies on HMEC-1 (Centers for Disease Control, Atlanta, GA, USA) Con A and chloroquine were incubated at a concentration of 15 μg ml^{-1} and 20 μM, respectively. Apoptotic cells were quantified by acridine orange and ethidium bromide staining as described elsewhere.[27] Phalloidin staining was performed as previously described.[28] Pictures were taken using a Nikon DN100 CCD camera mounted onto a Nikon Eclise E800 microscope (Nikon, Tokyo, Japan).

Flow cytometric analyses

$CD4^+$ cells were quantified by flow cytometry from fresh liver samples. Briefly, mice were killed 24h after Con A administration and liver lobes were dissected out, enzymatically and mechanically digested with collagenase (Sigma) into single cell suspensions. Additionally, cells were treated with red blood cell lysis buffer (0.15 M NH_4Cl, 1 mM $KHCO_3$, 0.1 mM

Na_2–EDTA) and, after hepatocyte sedimentation, supernatant was analyzed as described elsewhere.[29]

Transmigration and cell-adhesion assay

Cell adhesion was performed as previously described.[28] To analyze splenocytes transmigration through non-transfected, siSPARC or siSCR-lentivirus transfected HMEC-1 cell monolayers, pretreated for 3 h with Con A, a total number of 1×10^5 HMEC-1 cells were seeded on the top of 8 μm pore polycarbonate filters of 24-transwell units (Falcon, BD Labware) coated with 10 μg ml^{-1} fibronectin. HMEC-1 cells were allowed to attach overnight at 37 °C. CCL19 and CCL21 (10 ng μl^{-1}) were then placed in the lower chamber as splenocyte chemoattractants. 4,6-diamidino-2-phenylindole pre-stained splenocytes (5×10^5) were placed on the top of confluent HMEC-1 cells and were allowed to transmigrate for 4 h at 37 °C. After that, the membrane was carefully removed and cells on the upper side of the membrane were scraped off. Cells attached to the lower side of the membrane were fixed in 2% formaldehyde. Cells were counted using fluorescent-field microscopy and images captured in three representative visual fields (10x) were analyzed using CellProfiler software (www.cellprofiler.com), and the mean number of cells/field was obtained.

Electron microscopy

After 6 h, Con A-treated animals were killed and hepatic tissue dissected out and processed as described elsewhere.[30] Ultrathin sections (50 nm) were made and observed under a Hitachi H-7000 electron microscope (Hitachi, Tokyo, Japan).

Microarray analysis

Samples were processed following Microarrays Inc. (Nashville, USA) recommendations and aRNA was hybridized to 48.5 K exonic evidence-based oligonucleotide (HEEBO) arrays. The microarray signal intensity was evaluated using SpotReader software (Niles Scientific, Portola Valley, CA, USA). Normalization was performed in an R statistical environment using the Limma package (http://www.r-proyect.org). Raw data from the individual arrays were processed using standard and normexp background correction[31] and print-tip loess normalization.[32] For normalization in between arrays, the global scale normalization function with median absolute deviation was used.[33] Heatmaps were constructed using MeV software (TM4, Boston, MA, USA).[34] The gene ontology analysis was performed using DAVID Bioinformatics Resources 6.7 (http://david.abcc.ncifcrf.gov/),[35] and a pathway analysis was performed with the use of Ingenuity Pathway Analysis (Ingenuity Systems, www.ingenuity.com).

Statistical analysis

Data are expressed as mean ± s.e.m. Statistical analysis was performed using Fisher's least sgnificant difference test or Mann–Whitney or Dunn's multiple test when distribution was not normal. Differences were considered to be significant when $P < 0.05$. The results shown are mean values of three independent experiments.

Supplementary Material

Refer to Web version on PubMed Central for supplementary material.

Acknowledgments

We would like to thank V Ferreira, S Arregui and G Gastón for expert technical assistance This work was supported by grants from Austral University (for JB I04-12; for MGG T13-12; for JBA 17-09; and for GM T13-11) and from Agencia Nacional de Promoción Científica y Tecnológica (ANPCyT) grants PICT-2007/00082 (MGG and GM); PICT 2008/00123 (JBA); PICTO 2008/00122 (JBA); CTE-06 PIA CONICYT–Chile (MG and GM); PICTO 2008/00115 (MGG); PICT 2010/2818 (MGG and GM); PICT2008# and PICT 2011 # (MIC).

References

1. Bernuau J, Rueff B, Benhamou JP. Fulminant and subfulminant liver failure: definitions and causes. Semin Liver Dis. 1986; 6:97–106. [PubMed: 3529410]
2. Brekken RA, Sage EH. SPARC, a matricellular protein: at the crossroads of cell-matrix. Matrix Biol. 2000; 19:569–580. [PubMed: 11102747]
3. Bradshaw AD, Sage EH. SPARC, a matricellular protein that functions in cellular differentiation and tissue response to injury. J Clin Invest. 2001; 107:1049–1054. [PubMed: 11342565]
4. Atorrasagasti C, Peixoto E, Aquino JB, Kippes N, Malvicini M, Alaniz L, et al. Lack of the matricellular protein SPARC (secreted protein, acidic and rich in cysteine) attenuates liver fibrogenesis in mice. PLoS One. 2013; 8:e54962. [PubMed: 23408952]
5. Francki A, Bradshaw AD, Bassuk JA, Howe CC, Couser WG, Sage EH. SPARC regulates the expression of collagen type I and transforming growth factor-beta1 in mesangial cells. J Biol Chem. 1999; 274:32145–32152. [PubMed: 10542250]
6. Blazejewski S, Le Bail B, Boussarie L, Blanc JF, Malaval L, Okubo K, et al. Osteonectin (SPARC) expression in human liver and in cultured human liver myofibroblasts. Am J Pathol. 1997; 151:651–657. [PubMed: 9284812]
7. Kelly KA, Allport JR, Yu AM, Sinh S, Sage EH, Gerszten RE, et al. SPARC is a VCAM-1 counter-ligand that mediates leukocyte transmigration. J Leukoc Biol. 2007; 81:748–756. [PubMed: 17178915]
8. Murphy-Ullrich JE, Lane TF, Pallero MA, Sage EH. SPARC mediates focal adhesion disassembly in endothelial cells through a follistatin-like region and the Ca(2+)-binding EF-hand. J Cell Biochem. 1995; 57:341–350. [PubMed: 7539008]
9. Tiegs G, Hentschel J, Wendel A. A T cell-dependent experimental liver injury in mice inducible by concanavalin A. J Clin Invest. 1992; 90:196–203. [PubMed: 1634608]
10. Chang CP, Lei HY. Autophagy induction in T cell-independent acute hepatitis induced by concanavalin A in SCID/NOD mice. Int J Immunopathol Pharmacol. 2008; 21:817–826. [PubMed: 19144267]
11. Yang MC, Chang CP, Lei HY. Endothelial cells are damaged by autophagic induction before hepatocytes in Con A-induced acute hepatitis. Int Immunol. 2010; 22:661–670. [PubMed: 20547544]
12. Cardier JE, Schulte T, Kammer H, Kwak J, Cardier M. Fas (CD95, APO-1) antigen expression and function in murine liver endothelial cells: implications for the regulation of apoptosis in liver endothelial cells. FASEB J. 1999; 13:1950–1960. [PubMed: 10544178]
13. Ogasawara J, Watanabe-Fukunaga R, Adachi M, Matsuzawa A, Kasugai T, Kitamura Y, et al. Lethal effect of the anti-Fas antibody in mice. Nature. 1993; 364:806–809. [PubMed: 7689176]
14. De Caterina R, Libby P, Peng HB, Thannickal VJ, Rajavashisth TB, Gimbrone MA Jr, et al. Nitric oxide decreases cytokine-induced endothelial activation. Nitric oxide selectively reduces endothelial expression of adhesion molecules and proinflammatory cytokines. J Clin Invest. 1995; 96:60–68. [PubMed: 7542286]

15. Bykov I, Junnikkala S, Pekna M, Lindros KO, Meri S. Effect of chronic ethanol consumption on the expression of complement components and acute-phase proteins in liver. Clin Immunol. 2007; 124:213–220. [PubMed: 17586095]
16. Cain K, Freathy C. Liver toxicity and apoptosis: role of TGF-beta1, cytochrome c and the apoptosome. Toxicol Lett. 2001; 120:307–315. [PubMed: 11323189]
17. Knolle PA, Gerken G, Loser E, Dienes HP, Gantner F, Tiegs G, et al. Role of sinusoidal endothelial cells of the liver in concanavalin A-induced hepatic injury in mice. Hepatology. 1996; 24:824–829. [PubMed: 8855184]
18. Tang MJ, Tai IT. A novel interaction between procaspase 8 and SPARC enhances apoptosis and potentiates chemotherapy sensitivity in colorectal cancers. J Biol Chem. 2007; 282:34457–34467. [PubMed: 17897953]
19. Yiu GK, Chan WY, Ng SW, Chan PS, Cheung KK, Berkowitz RS, et al. SPARC (secreted protein acidic and rich in cysteine) induces apoptosis in ovarian cancer cells. Am J Pathol. 2001; 159:609–622. [PubMed: 11485919]
20. Bhoopathi P, Gondi CS, Gujrati M, Dinh DH, Lakka SS. SPARC mediates Src-induced disruption of actin cytoskeleton via inactivation of small GTPases Rho-Rac-Cdc42. Cell Signal. 2011; 23:1978–1987. [PubMed: 21798346]
21. Bai SW, Herrera-Abreu MT, Rohn JL, Racine V, Tajadura V, Suryavanshi N, et al. Identification and characterization of a set of conserved and new regulators of cytoskeletal organization, cell morphology and migration. BMC Biol. 2011; 9:54. [PubMed: 21834987]
22. Kim YC, Kim BG, Lee JH. Thymosin beta10 expression driven by the human TERT promoter induces ovarian cancer-specific apoptosis through ROS production. PLoS One. 2012; 7:e35399. [PubMed: 22623951]
23. Kaji N, Ohashi K, Shuin M, Niwa R, Uemura T, Mizuno K. Cell cycle-associated changes in Slingshot phosphatase activity and roles in cytokinesis in animal cells. J Biol Chem. 2003; 278:33450–33455. [PubMed: 12807904]
24. Ware CF, Sedy JR. TNF Superfamily Networks: bidirectional and interference pathways of the herpesvirus entry mediator (TNFSF14). Curr Opin Immunol. 2011; 23:627–631. [PubMed: 21920726]
25. Atorrasagasti C, Malvicini M, Aquino JB, Alaniz L, Garcia M, Bolontrade M, et al. Overexpression of SPARC obliterates the in vivo tumorigenicity of human hepatocellular carcinoma cells. Int J Cancer. 2010; 126:2726–2740. [PubMed: 19830689]
26. Camino AM, Atorrasagasti C, Maccio D, Prada F, Salvatierra E, Rizzo M, et al. Adenovirus-mediated inhibition of SPARC attenuates liver fibrosis in rats. J Gene Med. 2008; 10:993–1004. [PubMed: 18615449]
27. Piccioni F, Malvicini M, Garcia MG, Rodriguez A, Atorrasagasti C, Kippes N, et al. Antitumor effects of hyaluronic acid inhibitor 4-methylumbelliferone in an orthotopic hepatocellular carcinoma model in mice. Glycobiology. 2012; 22:400–410. [PubMed: 22038477]
28. Atorrasagasti C, Aquino JB, Hofman L, Alaniz L, Malvicini M, Garcia M, et al. SPARC downregulation attenuates the profibrogenic response of hepatic stellate cells induced by TGF-beta1 and PDGF. Am J Physiol Gastrointest Liver Physiol. 2011; 300:G739–G748. [PubMed: 21311029]
29. Malvicini M, Alaniz L, Bayo J, Garcia M, Piccioni F, Fiore E, et al. Single low-dose cyclophosphamide combined with interleukin-12 gene therapy is superior to a metronomic schedule in inducing immunity against colorectal carcinoma in mice. Oncoimmunology. 2012; 1:1038–1047. [PubMed: 23170252]
30. Luo Z, Liu H, Sun X, Guo R, Cui R, Ma X, et al. RNA interference against discoidin domain receptor 2 ameliorates alcoholic liver disease in rats. PLoS One. 2013; 8:e55860. [PubMed: 23409069]
31. Ritchie ME, Silver J, Oshlack A, Holmes M, Diyagama D, Holloway A, et al. A comparison of background correction methods for two-colour microarrays. Bioinformatics. 2007; 23:2700–2707. [PubMed: 17720982]
32. Smyth GK, Speed T. Normalization of cDNA microarray data. Methods. 2003; 31:265–273. [PubMed: 14597310]

33. Yang YH, Dudoit S, Luu P, Lin DM, Peng V, Ngai J, et al. Normalization for cDNA microarray data: a robust composite method addressing single and multiple slide systematic variation. Nucleic Acids Res. 2002; 30:e15. [PubMed: 11842121]

34. Saeed AI, Bhagabati NK, Braisted JC, Liang W, Sharov V, Howe EA, et al. TM4 microarray software suite. Methods Enzymol. 2006; 411:134–193. [PubMed: 16939790]

35. Huang da W, Sherman BT, Lempicki RA. Systematic and integrative analysis of large gene lists using DAVID bioinformatics resources. Nat Protoc. 2009; 4:44–57. [PubMed: 19131956]

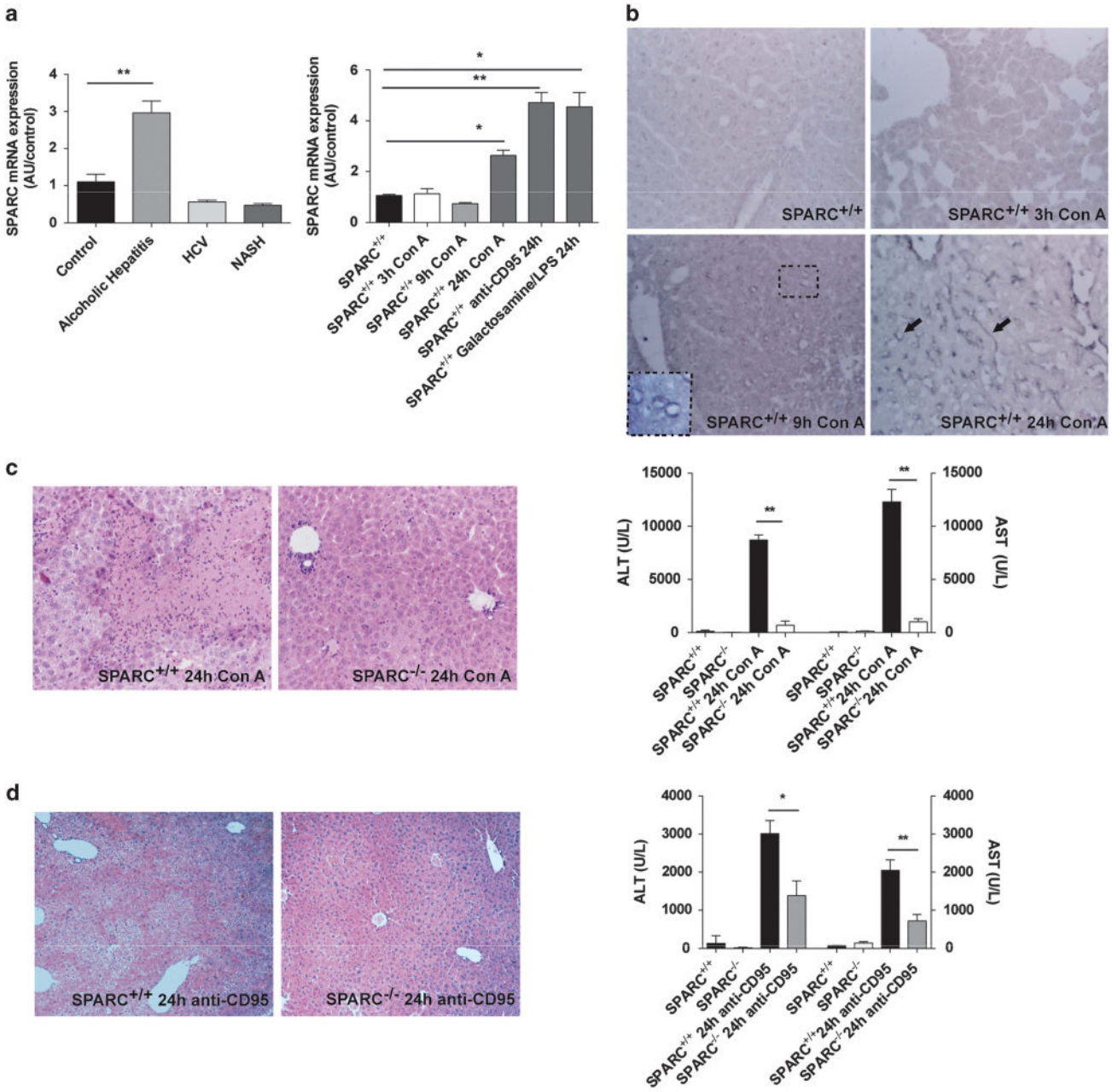

Figure 1.

Induction of SPARC expression during acute liver injury and SPARC-deficient mice protection from severe liver injury. (**a**) SPARC mRNA expression levels in human and mice liver samples as measured by qPCR. $^{**}P < 0.01$ versus control, Fisher's Data are expressed as mean ± s.e.m. Statistical analysis was performed using Fisher's least sgnificant difference test. $^{*}P < 0.05$, $^{**}P < 0.01$ versus SPARC$^{+/+}$, for Con A, Galactosamin/lipopolysaccharide or anti-CD95 treated mice, Dunn's multiple test. (**b**) Immunohistochemistry for SPARC. Arrows: endothelial location of SPARC expression (×200). (**c**) Hematoxylin and eosin (H&E) representative microphotographs (x400). Serum aspartate transaminase (AST) and alanine transaminase (ALT) levels; $P < 0.05$ SPARC$^{-/-}$ 24 h Con A versus SPARC$^{+/+}$ 24 h

Con A, Dunn's multiple test. (**d**) H&E representative microphotographs (×200). Serum AST and ALT after anti-CD95 application. *$P < 0.05$, **$P < 0.001$ $SPARC^{-/-}$ 24 h anti-CD95 versus $SPARC^{+/+}$ 24 h anti-CD95, Mann–Whitney test.

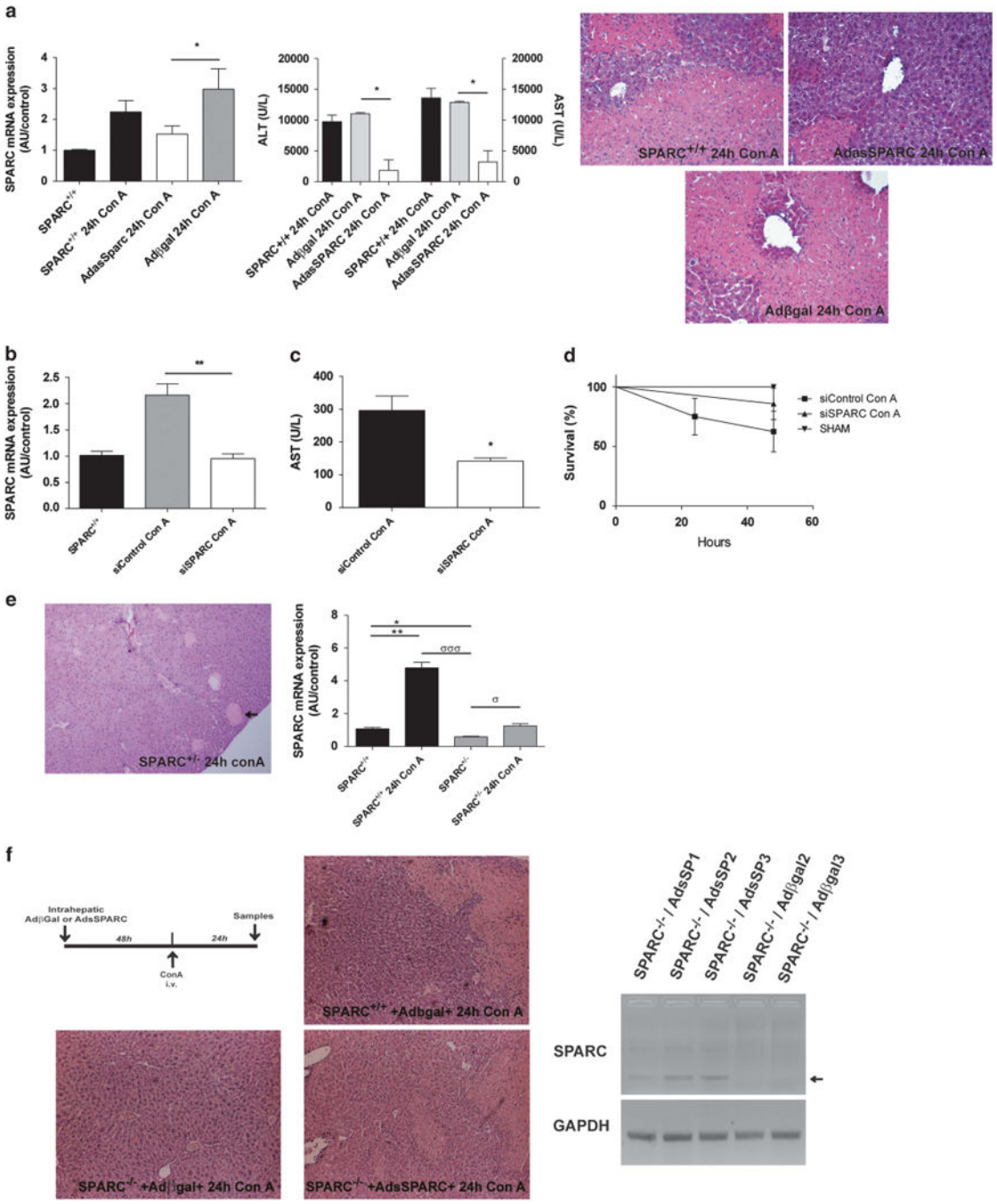

Figure 2.

Preventive and therapeutic effect of the attenuation of SPARC on Con A-induced severe liver injury. (**a**) quantitative PCR (qPCR) analyses of liver samples from untreated wild-type (wt), Con A-treated SPARC$^{+/+}$, Adβgal Con A-treated SPARC$^{+/+}$ or AdasSPARC SPARC$^{+/+}$ mice. *$P < 0.05$ versus Adβgal SPARC$^{+/+}$ 24 h Con A, Dunn's multiple test. Serum aspartate transaminase (AST) and alanine transaminase levels were measured after 24 h between Con A-treated SPARC$^{+/+}$, AdasSPARC SPARC$^{+/+}$ and Adβgal SPARC$^{+/+}$ groups. $P < 0.05$ versus SPARC$^{+/+}$ 24 h Con A, Dunn's multiple test. Hematoxylin and

eosin (H&E) microphotographs of liver sections from Con A-treated SPARC$^{+/+}$, AdasSPARC SPARC$^{+/+}$ and Adβgal SPARC$^{+/+}$ mice stained with H&E are also showed (x200). Therapeutic effect of siSPARC. (**b**) qPCR analyses of liver samples from untreated wt, siControl Con A-treated SPARC$^{+/+}$, or siSPARC SPARC$^{+/+}$ mice. *P < 0.01 versus siControl Con A, Dunn's multiple test. (**c**) Serum AST levels were measured after 48 h on siControl SPARC$^{+/+}$ and siSPARC SPARC$^{+/+}$ mice. P < 0.05 versus SPARC$^{+/+}$ 24 h Con A, Dunn's multiple test. (**d**) Survival curves of sham, siControl Con A-treated SPARC$^{+/+}$ or siSPARC SPARC$^{+/+}$ mice. P < 0.05, log-rank test. (**e**) H&E representative micrograph of liver sections from 24 h Con A-treated SPARC$^{+/-}$ mice (x100). qPCR analyses of liver samples from untreated, Con A-treated SPARC$^{+/+}$, untreated SPARC$^{+/-}$ and Con A-treated SPARC$^{+/-}$ mice. *P < 0.05, **P < 0.01 versus SPARC$^{+/+}$, σ < 0.05, σσσ < 0.001 versus SPARC$^{+/-}$, Dunn's multiple test. (**f**) H&E representative micrographs from 24 h Con A Adβgal SPARC$^{+/+}$, 24 h Con A Adβgal SPARC$^{-/-}$ and 24 h Con A AdsSPARC SPARC$^{-/-}$ mice (x200). SPARC expression RT-PCR of liver samples from 24 h Con A AdsSPARC SPARC$^{-/-}$, 24 h Con A Adβgal SPARC$^{-/-}$ mice.

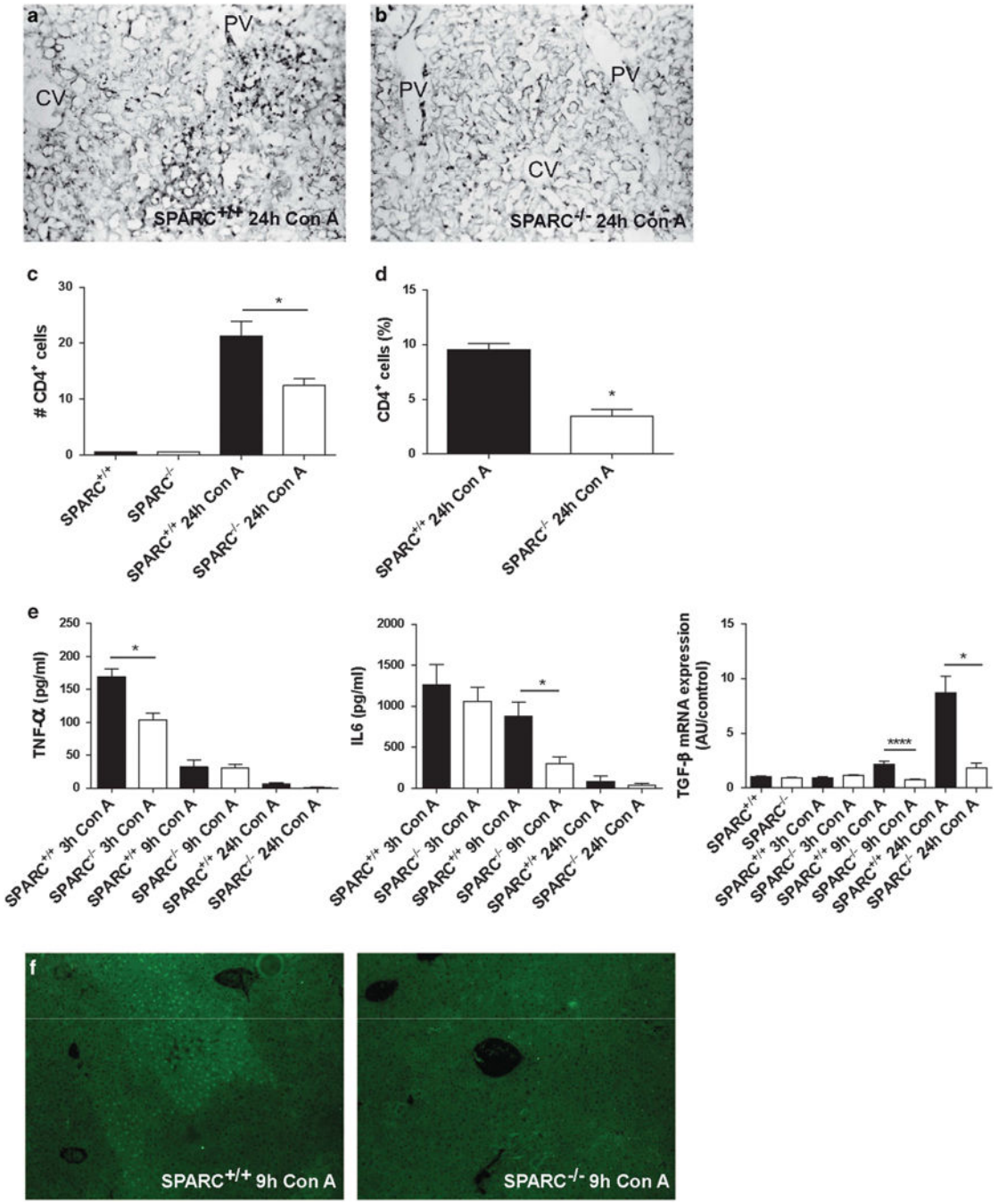

Figure 3.

Reduced parenchymal inflammatory infiltration and apoptosis in SPARC-deficient mice. (**a, b**) Immunohistochemistry for $CD4^+$ (x100). (**c**) Quantification of $CD4^+$ stained area. $*P <$ 0.05 $SPARC^{-/-}$ 24 h Con A versus $SPARC^{+/+}$ 24 h Con A, Dunn's multiple test. (**d**) Flow cytometry analysis of $CD4^+$ cells in the liver. $*P < 0.05$, Mann–Whitney test. (**e**) Serum levels of TNFα and interleukin-6 (IL-6). $*P < 0.05$ $SPARC^{-/-}$ 3 h Con A versus $SPARC^{+/+}$ 3 h Con A for TNFα and $SPARC^{-/-}$ 9 h Con A versus $SPARC^{+/+}$ 9 h Con A for IL-6, Mann–Whitney test. qPCR for TGF-β mRNA; $****P < 0.0001$ $SPARC^{-/-}$ 9 h Con A versus

SPARC$^{+/+}$ 9 h Con A and *P < 0.05 SPARC$^{-/-}$ 24 h Con A versus SPARC$^{+/+}$ 24 h Con A, Dunn's multiple test. (**f**) Representative microphotographs of liver sections from 9 h Con A-treated SPARC$^{+/+}$ or SPARC$^{-/-}$ mice stained using TUNEL assay (x40).

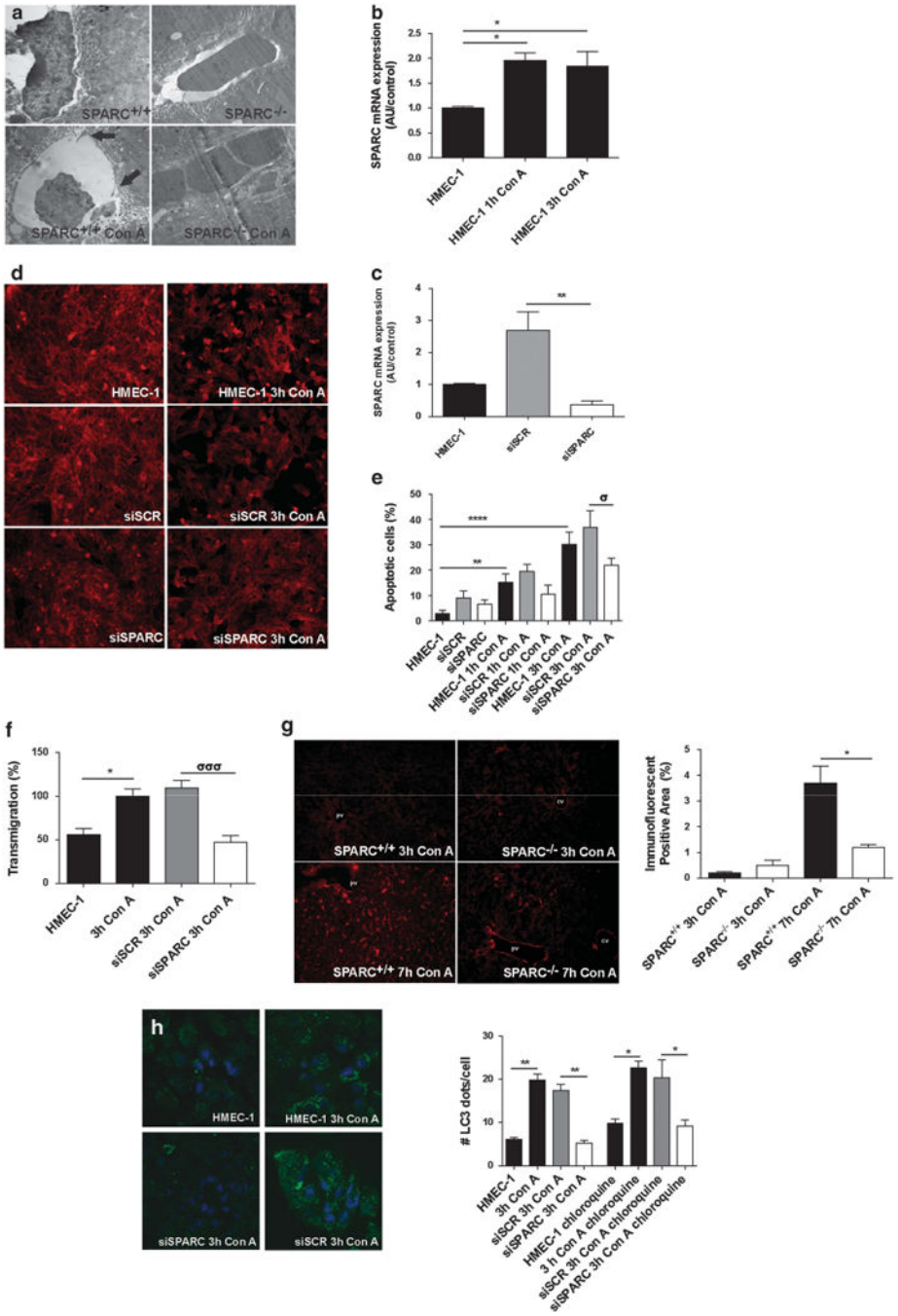

Figure 4.

Reduced alterations in endothelial cells after SPARC knockdown. (**a**) Representative electron micrographs of liver tissue sections of untreated SPARC$^{+/+}$, SPARC$^{-/-}$ and 6 h Con A-treated SPARC$^{+/+}$ and SPARC$^{-/-}$ mice. Arrows: damaged LSEC (x15000). (**b, c**) qPCR for SPARC expression on HMEC-1 cells. *$P < 0.05$, HMEC-1 1 and 3 h Con A versus untreated cells, Dunn's multiple test test. **$P < 0.01$, siSPARC versus siSCR, Mann–Whitney test. (**d**) Phalloidin staining of HMEC cells. (**e**) Apoptosis quantification of HMEC-1 cells by Con A incubation, using the AO/EB assay. **$P < 0.01$ HMEC-1 versuss

HMEC-1 1h Con A; ****$P < 0.0001$ HMEC-1 versus HMEC-1 3 h Con A; $^{\sigma}P < 0.05$, siSCR 3 h Con A versus siSPARC 3 h Con A, Mann–Whitney test. (**f**) Splenocytes-HMEC-1 layer transmigration assay. Mean values ± s.e.m. for individual groups are shown. *$P < 0.05$ HMEC-1 versus HMEC-1 3 h Con A, σσσ$P < 0.01$ siSCR 3 h Con A versus siSPARC 3 h Con A, Dunn's multiple test. (**g**) Immunofluorescence for VCAM-1 (x200) pv, portal vein; cv, central vein. *$P < 0.05$ $SPARC^{+/+}$ 7 h Con A versus $SPARC^{-/-}$ 7 h Con A, Dunn's multiple test. (**h**) LC3 dots per HMEC-1 cell (x600); **$P < 0.01$, HMEC-1 versus 3 h Con A, siSCR 3 h Con A versus siSPARC 3 h Con A; *$P < 0.05$, HMEC-1 chloroquine versus 3 h Con A chloroquine, siSCR 3 h Con A chloroquine versus siSPARC 3 h Con A chloroquine, Dunn's multiple comparisons test.

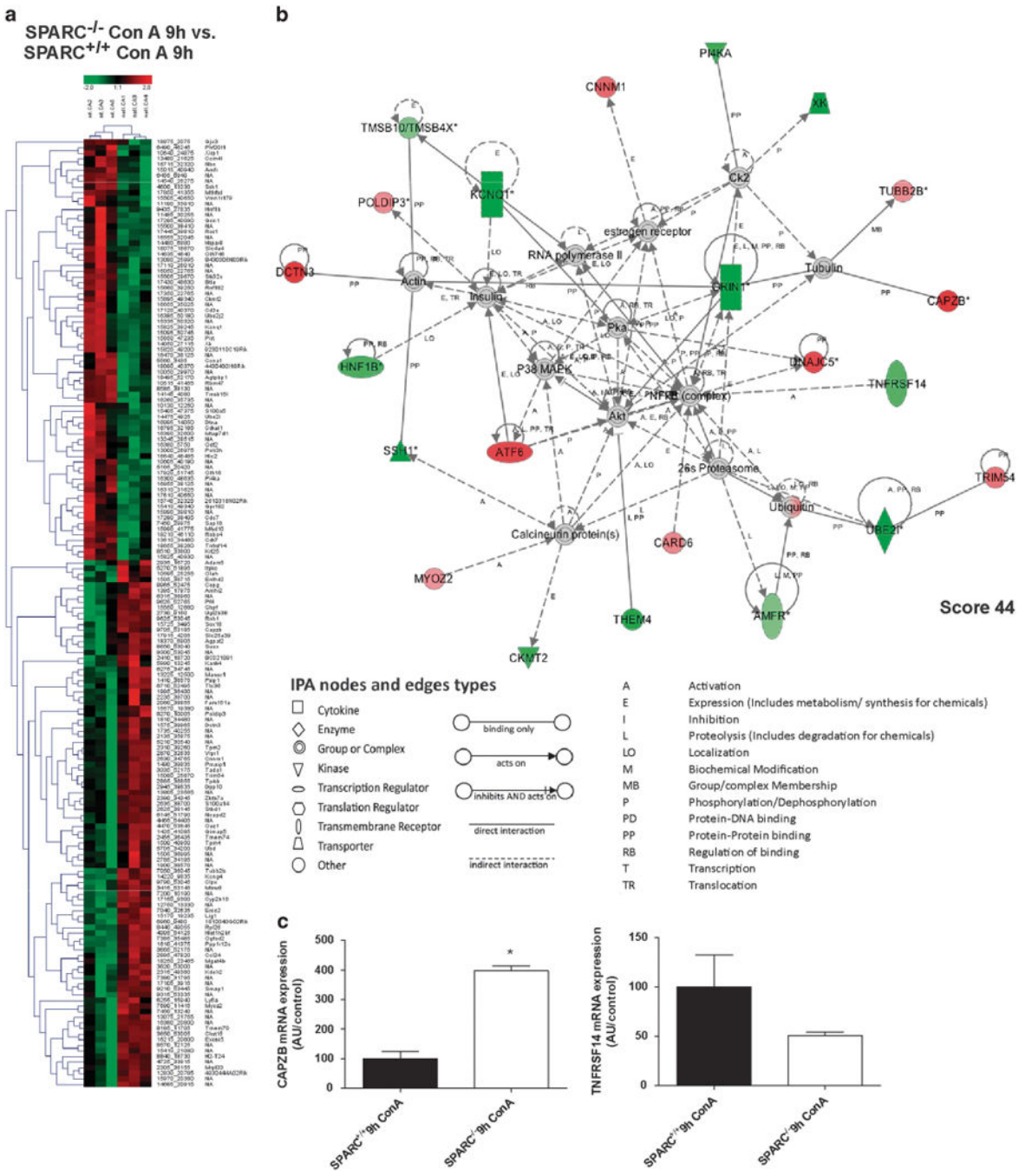

Figure 5.

Heatmap and top network of differentially expressed genes. (**a**) Heatmap of differential gene expression among experimental groups at 9 h after Con A application. (**b**) Top network of differentially expressed genes in between SPARC$^{-/-}$ and SPARC$^{+/+}$ after 9 h of Con A treatment, as identified by Ingenuity Pathway Analysis (IPA) analysis. Upregulated and downregulated genes in SPARC$^{-/-}$ mice are shown as red spot or green spot, respectively. Intensity of the red or green color shows the level of gene expression. Gray represents a gene found which is related to the others, but did not meet the cut off criteria. (**c**) CAPZB

and TNFRSF14 mRNA expression levels on mice liver samples after 9 h Con A injection. *$P < 0.05$. Mann–Whitney test.

Table 1

Ingenuity Pathway Analysis (IPA) top molecules that were differentially expressed in SPARC$^{-/-}$ versus SPARC$^{+/+}$ 9 h Con A-treated mice

	Gene ID	*Exponential value*
Fold change upregulated		
CLPX	NM_011802	2.519
PF4	NM_019932	2.455
RNH1	NM_145135	2.411
FAM151A	NM_146149	2.337
OLAH	NM_145921	2.310
GIMAP1-GIMAP5	NM_175035	2.224
CAPZB	NM_009798	2.153
Tpm4	NM_001001491	2.059
C8G	XM_130127	2.057
GYS1	NM_008195	2.055
Fold change downregulated		
STK32C	NM_021302	− 3.318
CCRN4L	NM_009834	− 2.747
PIRT	NM_178656	− 2.485
C11orf70	NM_199017	− 2.399
HIC2	NM_178922	− 2.356
Scgb2b26/Scgb2b27	NM_194338	− 2.338
RNF182	NM_183204	− 2.309
GJC3	NM_080450	− 2.281
BRD8	NM_144864	− 2.222
9830107B12Rik (includes others)	NM_177083	−2.068

IPA top molecules. 9 h of Con A treatment.

Table 2

qPCR Primers

Target gene	*Sense primer*	*Antisense primer*
SPARC mouse	5′-CCACACGTTTCTTTGAGACC-3′	5′-AAACCGAAGAGGAGGTGGTG-3′
SPARC human	5′-GGGGCTGCCCAGAACATCAT-3′	5′-ACCAACTATTGCTTCAGCTC-3′
GAPDH	5′-GATGTCCTGCTCCTTGATGC-3′	5′-GCAAAGAAGTGGCAGGAAGA-3′
TGF-β1	5′-GCCTGCTTCACCACCTTCTTG-3′	5′-TGTTGGTTGTAGAGGGCAAG-3′

Abbreviations: GADPH, glyceraldehyde 3-phosphate dehydrogenase; SPARC, secreted protein, acidic and rich in cysteine; TGF-β1, transforming growth factor-β1.